OCS Study
MMS 2000-052

FINAL REPORT

ENVIRONMENTAL SURVEY OF POTENTIAL SAND RESOURCE SITES: OFFSHORE NEW JERSEY

Volume I: Main Text

Prepared by:

Applied Coastal Research and Engineering, Inc.
766 Falmouth Road, Suite A-1
Mashpee, MA 02649

In Cooperation With:

Continental Shelf Associates, Inc.
Barry A. Vittor & Associates, Inc.
Aubrey Consulting, Inc.

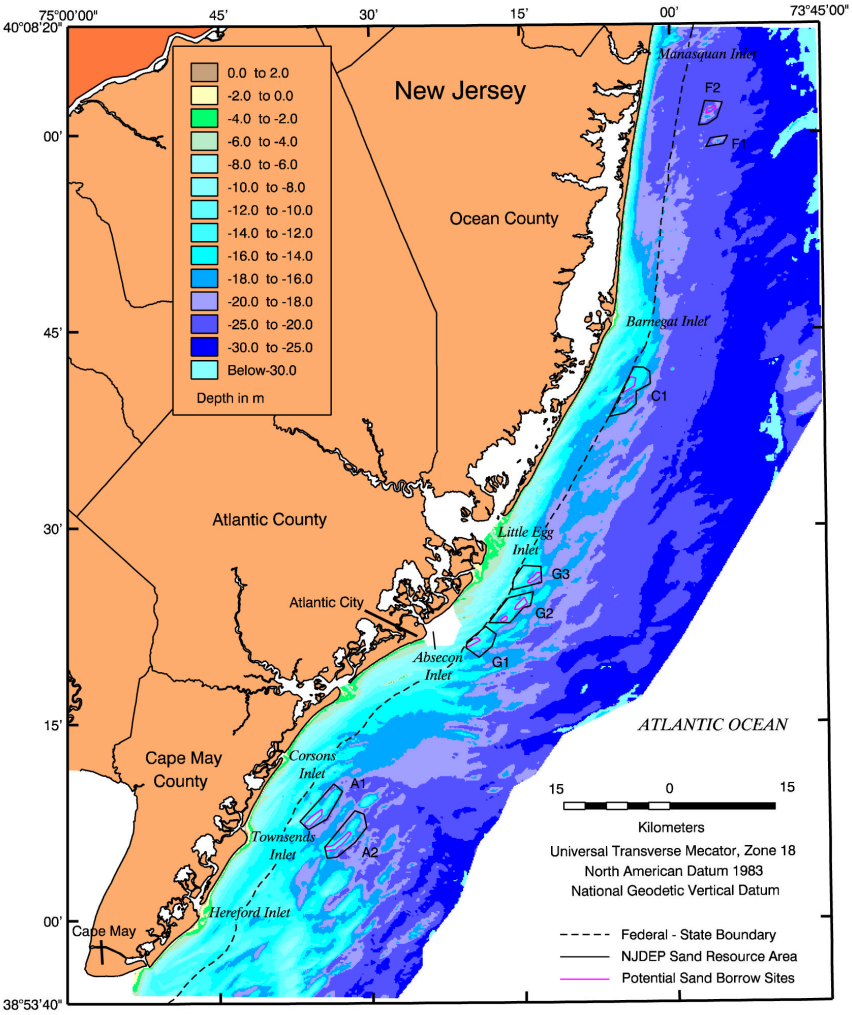

Prepared for:

U.S. Department of the Interior
Minerals Management Service
International Activities and Marine Minerals Division (INTERMAR)

Funded Under Contract Number 14-35-01-97-CT-30864

DISCLAIMER

This report has been reviewed by the Minerals Management Service and approved for publication. Approval does not signify that the contents necessarily reflect the views and policies of the Service, nor does mention of trade names or commercial products constitute endorsement or recommendation for use.

SUGGESTED CITATION

Byrnes, M.R., R.M. Hammer, B.A. Vittor, J.S. Ramsey, D.B. Snyder, J.D. Wood, K.F. Bosma, T.D. Thibaut, N.W. Phillips, 2000. Environmental Survey of Potential Sand Resource Sites: Offshore New Jersey. U.S. Department of the Interior, Minerals Management Service, International Activities and Marine Minerals Division (INTERMAR), Herndon, VA. OCS Report MMS 2000-052, Volume I: Main Text 380 pp. + Volume II: Appendices 291 pp.

FINAL REPORT

Environmental Survey Of Potential Sand Resource Sites: Offshore New Jersey

December 2000

Mark R. Byrnes
Physical Processes Project Manager, Co-Editor
(Applied Coastal Research and Engineering, Inc.)

Richard M. Hammer
Biological Component Project Manager, Co-Editor
(Continental Shelf Associates, Inc.)

With Contributions From:

Barry A. Vittor
Barry A. Vittor & Associates, Inc.

John S. Ramsey
Applied Coastal Research and Engineering, Inc.

David B. Snyder
Continental Shelf Associates, Inc.

Jon D. Wood
Applied Coastal Research and Engineering, Inc.

Kirk F. Bosma
Aubrey Consulting, Inc.

Tim D. Thibaut
Barry A. Vittor & Associates, Inc.

Neal W. Phillips
Continental Shelf Associates, Inc.

Prepared by:
Applied Coastal Research and Engineering, Inc.
766 Falmouth Road, Suite A-1
Mashpee, MA 02649

Prepared for:
U.S. Department of the Interior
Minerals Management Service
International Activities and Marine Minerals Division (INTERMAR)
381 Elden Street, MS 4030
Herndon, VA 22070

In Cooperation With:
Continental Shelf Associates, Inc.
Barry A. Vittor & Associates, Inc.
Aubrey Consulting, Inc.

Contract Number 14-35-01-97-CT-30864

ACKNOWLEDGMENTS

Numerous people contributed to the project titled *Environmental Survey of Potential Sand Resource Sites: Offshore New Jersey*, which was funded by the U.S. Department of the Interior, Minerals Management Service (MMS), International Activities and Marine Minerals Division (INTERMAR). Mr. Barry S. Drucker provided assistance and direction during the project as the MMS Contracting Officer's Technical Representative. Ms. Jane Carlson served as the MMS Contracting Officer. Mr. Barry Drucker and Mr. Roger Amato of the MMS reviewed the draft document.

Dr. Mark R. Byrnes of Applied Coastal Research and Engineering, Inc. (Applied Coastal) served as Project Manager; Physical Processes Component Manager; authored Sections 1.0 (Introduction), 2.1 (Offshore Sedimentary Environment), 7.1 (Offshore Sand Resource Areas), 7.4.1 (Historical Sediment Transport Patterns), and Section 3.0 (Regional Geomorphic Change); co-authored with Dr. Richard M. Hammer Sections 7.7 (Potential Cumulative Effects), 8.0 (Conclusions); and was Co-Editor of the report. Dr. Richard M. Hammer of Continental Shelf Associates, Inc. (CSA) served as the Biological Component Manager, authored Sections 7.5.1 (Effects of Offshore Dredging on Benthic Fauna) and 7.5.2 (Recolonization Rate and Success), and was Co-Editor of the report.

Other Applied Coastal personnel who participated in the project included Mr. John S. Ramsey who led the nearshore sediment transport modeling component of the study. Mr. Ramsey authored Sections 2.2.5 (Nearshore Sediment Transport), 5.2.2 (Nearshore Sediment Transport Modeling), and 7.4.3 (Nearshore Sediment Transport Trends). Mr. Jon D. Wood authored Sections 5.1.1 (Historical Data Analysis), 5.1.2 (Summary of Flow Regimes at Offshore Borrow Sites), 7.3 (Currents and Circulation), and co-authored Section 2.2 (General Circulation). Ms. Feng Li was responsible for shoreline and bathymetry change data compilation and surface modeling. Ms. Jessica M. Côté assisted with data analysis and report preparation related to currents and circulation, and nearshore sediment transport modeling. Ms. Elizabeth A. Wadman was responsible for report compilation and editorial assistance during production of the report.

Additional CSA personnel who contributed to the project included Mr. David B.Snyder who served as Chief Scientist during Biological Field Survey 2; authored Sections 2.3.1.2 and 7.5.4 (Atlantic Surf Clam), 2.3.2.1 and 7.6.1 (Zooplankton), 2.3.2.2 and 7.6.2 (Squids), and 2.3.2.3 and 7.6.3 (Fishes); and incorporated sections from other authors concerning infauna, epifauna and demersal fishes, and discussion into the remainder of Section 6.0 (Biological Field Surveys) that he authored. Dr. Alan D. Hart led the sampling design and statistical analyses for the biological data. Dr. Neal W. Phillips wrote Sections 2.3.2.4 and 7.6.4 (Sea Turtles) and 2.3.2.5 and 7.6.5 (Marine Mammals). Mr. Paul S. Fitzgerald served as Chief Scientist during Field Survey 1 and Scientist for Survey 2. Mr. Thomas Quinney served as Scientist during Survey 1. Mr. Frederick B. Ayer, III directed the field surveys and pre-plotted the station locations. Mr. Lynwood R. Powell, Jr. produced the field survey post-plot figures. Ms. Melody Powell provided editorial assistance and supervised CSA support staff during production of the report.

Personnel from Aubrey Consulting, Inc. who contributed to the project included Mr. Kirk F. Bosma who led the wave transformation numerical modeling effort and co-authored Sections 4.0 (Wave Transformation Numerical Modeling), 5.1.3 (Wave-Induced Bottom Currents), 5.1.4 (Wave-Generated Currents), 5.2.1 (Sediment Transport at Borrow Sites), 7.2 (Wave Transformation), and 7.4.2 (Sediment Transport at Potential Borrow Sites). Mr. Steven Jachec provided technical assistance on Sections 4.0 (Wave Transformation Numerical Modeling) and 5.2.1 (Sediment Transport at Borrow Sites). Ms. Nadine Sweeney provided editorial assistance for the ACI portion of the report. Mr. Ken Israel and Dr. Dave Cacchione provided technical assistance on Section 5.1 (Currents and Circulation).

Personnel from Barry A. Vittor & Associates, Inc. (BVA) who contributed to the project included Dr. Barry A. Vittor, who served as Manager of BVA's responsibilities for the field surveys and report. Mr. Tim D. Thibaut authored Sections 2.3.1.1 and 6.3.3 (Infauna), 2.3.1.3 and 6.3.4 (Epifauna and Demersal Fishes), 6.4 (Discussion), and 7.5.3 (Predictions Relative to the Sand Resource Areas) of the report, with assistance from Dr. Vittor. Mr. J. Dobbs Lee served as Scientist during both field surveys. Mr. Joie M. Horn served as Scientist during Survey 2. Ms. Linda W. Sierke supervised personnel associated with taxonomic identifications. Mr. Felix Fernandez served as Manager for BVA's benthic infaunal data entry and analysis.

Dr. Wayne C. Isphording, from the University of South Alabama, was responsible for the laboratory grain size analyses. Dr. Rober J. Diaz and Mr. G. Randall Cutter Jr., from the Virginia Institute of Marine Science, conducted the sediment profiling camera aspects of the project.

TABLE OF CONTENTS

1.0 INTRODUCTION 1

1.1 STUDY AREA AND BORROW SITE CHARACTERISTICS 2
1.2 STUDY PURPOSE 5
1.3 STUDY APPROACH 6
1.3.1 Baseline Ecological Conditions 7
1.3.2 Benthic Infaunal Evaluation 7
1.3.3 Project Scheduling 7
1.3.4 Wave Modifications 7
1.3.5 Sediment Transport Patterns 7
1.4 DOCUMENT ORGANIZATION 8

2.0 EXISTING LITERATURE 9

2.1 OFFSHORE SEDIMENTARY ENVIRONMENT 10
2.1.1 Seabed Morphology 14
2.1.2 Surface Sediments 16
2.1.3 Subsurface Deposits 21
2.1.4 Sand Resource Areas 29
2.2 GENERAL CIRCULATION 35
2.2.1 Tidal Currents 36
2.2.2 Monthly Mean Currents 36
2.2.3 Low-Frequency Synoptic-Scale Currents 36
2.2.4 Water Level Variations 37
2.2.5 Nearshore Sediment Transport 37
2.3 BIOLOGY 38
2.3.1 Benthic Environment 38
2.3.1.1 Infauna 38
2.3.1.2 Atlantic Surfclam 43
2.3.1.3 Epifauna and Demersal Fishes 43
2.3.2 Pelagic Environment 47
2.3.2.1 Zooplankton 47
2.3.2.2 Squids 53
2.3.2.3 Fishes 53
2.3.2.4 Sea Turtles 55
2.3.2.5 Marine Mammals 57

3.0 REGIONAL GEOMORPHIC CHANGE 60

3.1 SHORELINE POSITION CHANGE 60
3.1.1 Previous Studies 60
3.1.2 Shoreline Position Data Base 61
3.1.3 Historical Change Trends 65
3.1.3.1 1839/42 to 1932 66
3.1.3.2 1932 to 1977 73
3.1.3.3 Cumulative Shoreline Position Change (1839/42 to 1977) 73
3.2 NEARSHORE BATHYMETRY CHANGE 79
3.2.1 Bathymetry Data Base and Potential Errors 79
3.2.2 Digital Surface Models 81
3.2.2.1 1843/91 Bathymetric Surface 82

3.2.2.2 1934/77 Bathymetric Surface 82
3.2.3 Shelf Sediment Transport Dynamics 85
3.2.4 Magnitude and Direction of Change 87
3.2.5 Net Longshore Sand Transport Rates 87
3.3 SUMMARY 90

4.0 WAVE TRANSFORMATION NUMERICAL MODELING 91

4.1 ANALYSIS APPROACH 91
4.1.1 Wave Model Description 91
4.1.2 Required Input Conditions 93
4.2 WAVE CHARACTERISTICS AND INPUT SPECTRA 93
4.2.1 Wave Data Analysis and Sources 93
4.2.1.1 Wave Information Study and Additional Data Sources 93
4.2.1.2 Data Comparison 96
4.2.1.3 Wave Direction Characteristics 97
4.2.1.4 High Energy Events 102
4.2.2 Input Condition Parameters 103
4.2.2.1 Spectra Development 103
4.2.2.2 Selection of Wave Conditions 103
4.2.3 High Energy Event Parameters 104
4.3 GRID GENERATION 106
4.3.1 Existing Conditions 106
4.3.2 Post-Dredging Scenarios 111
4.3.2.1 Sand Borrow Site Selection 111
4.3.2.2 Numerical Excavation of Gridded Surfaces 111
4.4 PRE-DREDGING RESULTS 112
4.4.1 Grid A Simulations 112
4.4.1.1 Directional Approach Simulations 112
4.4.1.2 High Energy Wave Events Simulations 120
4.4.1.3 Model Results Relative to Historical Shoreline Change 122
4.4.2 Grid B1 Simulations 125
4.4.2.1 Directional Approach Simulations 125
4.4.2.2 High Energy Wave Events Simulations 133
4.4.2.3 Model Results Relative to Historical Shoreline Change 134
4.4.3 Grid B2 Simulations 137
4.4.3.1 Directional Approach Simulations 137
4.4.3.2 High Energy Wave Events Simulations 145
4.4.3.3 Model Results Relative to Historical Shoreline Change 145
4.4.4 Grid C Simulations 149
4.4.4.1 Directional Approach Simulations 149
4.4.4.2 High Energy Wave Events Simulations 157
4.4.4.3 Model Results Relative to Historical Shoreline Change 159
4.5 COMPARISON OF PRE- AND POST-DREDGING RESULTS 162
4.5.1 Grid A Simulations 162
4.5.1.1 Post-Dredging Results 162
4.5.1.2 Existing Conditions Versus Post-Dredging Seasonal Results 163
4.5.1.3 High Energy Wave Event Results 165
4.5.2 Grid B1 Simulations 167
4.5.2.1 Post-Dredging Results 167
4.5.2.2 Existing Conditions Versus Post-Dredging Seasonal Results 168

4.5.2.3 High Energy Wave Event Results 170
4.5.3 Grid B2 Simulations 172
4.5.3.1 Post-Dredging Results 172
4.5.3.2 Existing Conditions Versus Post-Dredging Seasonal Results 172
4.5.3.3 High Energy Wave Event Results 174
4.5.4 Grid C Simulations 177
4.5.4.1 Post-Dredging Results 177
4.5.4.2 Existing Conditions Versus Post-Dredging Seasonal Results 178
4.5.4.3 High Energy Wave Event Results 179
4.6 DISCUSSION 182

5.0 CIRCULATION AND SEDIMENT TRANSPORT DYNAMICS 184

5.1 CURRENTS AND CIRCULATION 184
5.1.1 Historical Data Analysis 184
5.1.1.1 Description of Observed Currents 184
5.1.1.2 Numerical Decomposition of Observed Currents 185
5.1.1.3 Current Components 186
5.1.1.4 Seasonal Variability 188
5.1.2 Summary of Flow Regimes at Offshore Borrow Sites 191
5.1.3 Wave-Induced Bottom Currents 191
5.1.4 Wave-Induced Longshore Currents 193
5.1.4.1 Governing Equations 194
5.1.4.2 Lateral Mixing 196
5.1.4.3 Model Verification 197
5.1.4.4 Wave-Induced Currents Along the New Jersey Coast 198
5.2 SEDIMENT TRANSPORT MODELING 203
5.2.1 Sediment Transport at Borrow Sites 203
5.2.1.1 Initiation of Sediment Motion Under Combined Wave and Current Action 203
5.2.1.2 Relative Magnitude and Direction of Transport 203
5.2.1.3 Hydrodynamics and Sediment Transport for Resource Areas A1 and A2 207
5.2.1.4 Hydrodynamics and Sediment Transport for Resource Area C1 (Grid B1) 214
5.2.1.5 Hydrodynamics and Sediment Transport for Resource Areas G2 and G3 (Grid B2) 218
5.2.1.6 Hydrodynamics and Sediment Transport for Resource Area F2 (Grid C) 227
5.2.1.7 Annual Sediment Transport Magnitude and Direction, and Infilling Times 232
5.2.2 Nearshore Sediment Transport Modeling 233
5.2.2.1 Model Development 233
5.2.2.2 Sediment Transport Along the New Jersey Coast 234
5.2.2.3 Nearshore Sediment Transport Versus Historical Shoreline Change 243

6.0 BIOLOGICAL FIELD SURVEYS 253

6.1 BACKGROUND 253
6.2 METHODS 253
6.2.1 Survey Design 253
6.2.2 Field Methods 266
6.2.2.1 Vessel 266
6.2.2.2 Navigation 266
6.2.2.3 Water Column 266
6.2.2.4 Sediment Grain Size 266
6.2.2.5 Infauna 267

6.2.2.6 Epifauna and Demersal Fishes 267
6.2.3 Laboratory Methods 267
6.2.3.1 Sediment Grain Size 267
6.2.3.2 Infauna 267
6.2.4 Data Analysis 267
6.2.4.1 Water Column 267
6.2.4.2 Sediment Grain Size 267
6.2.4.3 Infauna 268
6.2.4.4 Epifauna and Demersal Fishes 269
6.3 RESULTS 269
6.3.1 Water Column 269
6.3.2 Sediment Grain Size 274
6.3.3 Infauna 274
6.3.4 Epifauna and Demersal Fishes 297
6.4 DISCUSSION 300

7.0 POTENTIAL EFFECTS 305

7.1 OFFSHORE SAND RESOURCE AREAS 305
7.2 WAVE TRANSFORMATION 306
7.3 CURRENTS AND CIRCULATION 307
7.4 SEDIMENT TRANSPORT 308
7.4.1 Historical Sediment Transport Patterns 309
7.4.2 Sediment Transport at Potential Borrow Sites 310
7.4.3 Nearshore Sediment Transport Trends 310
7.4.3.1 Grid A 313
7.4.3.2 Grid B2 313
7.4.3.3 Grid B1 316
7.4.3.4 Grid C 316
7.4.3.5 50-Year Storm Conditions 319
7.4.3.6 Significance of Transport Trends 319
7.5 BENTHIC ENVIRONMENT 324
7.5.1 Effects of Offshore Dredging on Benthic Fauna 325
7.5.1.1 Sediment Removal 325
7.5.1.2 Sediment Suspension/Dispersion 326
7.5.1.3 Sediment Deposition 327
7.5.2 Recolonization Rate and Success 328
7.5.2.1 Adaptations for Recolonization and Succession 328
7.5.2.2 Successional Stages 328
7.5.2.3 Recolonization Rates 330
7.5.2.4 Recolonization Success and Recovery 331
7.5.3 Predictions Relative to the Sand Resource Areas 333
7.5.3.1 Potential Benthic Effects 333
7.5.3.2 Potential Recolonization Rate and Success 335
7.5.4 Atlantic Surfclam 337
7.5.4.1 Entrainment 337
7.5.4.2 Hypoxia/Anoxia 337
7.5.4.3 Turbidity 337
7.5.4.4 Project Scheduling 337
7.6 PELAGIC ENVIRONMENT 338
7.6.1 Zooplankton 338

7.6.1.1 Entrainment 338
7.6.1.2 Turbidity 338
7.6.1.3 Project Scheduling 339
7.6.2 Squids 340
7.6.2.1 Entrainment 340
7.6.2.2 Attraction 340
7.6.2.3 Project Scheduling 340
7.6.3 Fishes 341
7.6.3.1 Entrainment 341
7.6.3.2 Attraction 341
7.6.3.3 Turbidity 341
7.6.3.4 Project Scheduling 341
7.6.3.5 Essential Fish Habitat 342
7.6.4 Sea Turtles 342
7.6.4.1 Entrainment 342
7.6.4.2 Habitat Modification 344
7.6.4.3 Turbidity 344
7.6.4.4 Hypoxia/Anoxia 344
7.6.4.5 Noise 344
7.6.4.6 Project Scheduling Considerations 345
7.6.5 Marine Mammals 345
7.6.5.1 Physical Injury 345
7.6.5.2 Turbidity 345
7.6.5.3 Noise 345
7.6.5.4 Project Scheduling Considerations 346
7.7 POTENTIAL CUMULATIVE EFFECTS 346

8.0 CONCLUSIONS 347

8.1 WAVE TRANSFORMATION MODELING 347
8.2 CIRCULATION AND SEDIMENT TRANSPORT DYNAMICS 348
8.2.1 Historical Sediment Transport Patterns 349
8.2.2 Sediment Transport at Potential Borrow Sites 350
8.2.3 Nearshore Sediment Transport Modeling 351
8.3 BENTHIC ENVIRONMENT 352
8.4 PELAGIC ENVIRONMENT 353
8.5 SYNTHESIS 354

9.0 LITERATURE CITED 355

APPENDICES

APPENDIX A. HIGH-WATER SHORELINE POSITION CHANGE A1

APPENDIX B. WAVE TRANSFORMATION NUMERICAL MODELING B1

B1. Wave Model Theoretical Background B2
B2. Spectra Development B9
B3. Directional and Frequency Verification B10
B4. Wave Transformation Compared with Historical Shoreline Change B19
B5. Post-Dredging Wave Transformation Results B29
B6. Pre- and Post-Dredging Difference Plots B44

APPENDIX C. SEDIMENT TRANSPORT NUMERICAL MODELING C1

C1. Initiation of Sediment Motion Under Combined Wave and Current Action C2
C2. Relative Magnitude and Direction of Transport C7
C3. Longshore Sediment Transport Model Results C9

APPENDIX D. BIOLOGICAL FIELD SURVEY DATA D1

D1. Sediment Profiling Camera Data D2
D2. Sample Types, Sample Codes, Coordinates, and Water Depths D52
D3. Hydrolab Data D62
D4. Sediment Grain Size Data D67
D5. Infaunal Data D73

LIST OF FIGURES

Figure 1-1. Location diagram illustrating sand resource areas and the Federal-State boundary relative to the 1934/77 bathymetry. 3
Figure 2-1. Coastal New Jersey and vicinity (from Smith, 1996). 9
Figure 2-2. Map of the Atlantic continental shelf illustrating the dominant surface sedimentary facies as >75% sand sized material (from Duane and Stubblefield, 1988). 11
Figure 2-3. A summary of the: A) Pleistocene-Holocene paleoenvironments of the Middle Atlantic Province and B) sedimentary facies for the same area. Data from Emery and Uchupi, 1965; Uchupi, 1968; Swift, 1976. Figure from Duane and Stubblefield (1988). 12
Figure 2-4. Sand ridge orientations for the New Jersey continental shelf. Each division on the x-y axis of the rose diagrams represents a value of two, and the compass rose is divided into 10° units. The study area includes regions A, C, F, and G (from Stubblefield et al., 1984). 13
Figure 2-5. Distribution of shoreface sand ridges and tidal inlets for the New Jersey coast (from McBride and Moslow, 1991). 14
Figure 2-6. Average ridge azimuth (orientation), wavelength (spacing), width, and height for sand ridges on the New Jersey continental shelf (from Stubblefield et al., 1984). 15
Figure 2-7. Surficial sediment texture on the New Jersey continental shelf (from Poppe et al., 1994). Yellow areas represent sand (sd) and orange areas depict gravelly sand (gr-sd) deposits. 17
Figure 2-8. Pattern of mean grain size (moment statistic) for offshore sediment between southern Long Beach Island and Absecon Inlet, New Jersey (from Frank and Friedman, 1973). Depth contours are in fathoms. 18
Figure 2-9. Surface sediment sample locations on the New Jersey continental shelf (from Donahue et al., 1966). 19
Figure 2-10. Median diameter (Md), grain sorting (So), and $\log_{10}$ skewness (Sk) for surface sediment samples illustrated in Figure 2-8 (from Donahue et al., 1966). 19
Figure 2-11. A) Index map illustrating two sediment grab sample transects over nearshore and middle shelf sand ridges. B) Plot of mean grain size across the nearshore and middle shelf sand ridge (from Stubblefield and Swift, 1981). 20
Figure 2-12. Study area locations for McClennen (1983; thick solid line), Alpine Ocean Seismic Survey (1988; dashed line), and Ashley et al. (1991; dash-dot line) (study locations from Uptegrove et al., 1995). 23
Figure 2-13. Study area locations for Miller et al. (1973; dashed line) and Meisburger and Williams (1982; thick solid line) (study locations from Uptegrove et al., 1995). 24
Figure 2-14. General location diagram for U.S. Army Corps of Engineers (USACE) central New Jersey sand resource study area (from Meisburger and Williams, 1982). 25
Figure 2-15. Map of U.S. Army Corps of Engineers (USACE) sand resource sites (dark blue lines labeled D, G, H, I, J, K, L) relative to New Jersey Geological Survey (NJGS) sand resource areas (labeled A1, A2, G1, G2, G3, C, F1, F2). Sand resource locations are from Meisburger and Williams (1982) and the NJGS. 26

Figure 2-16. Study area locations for Meisburger and Williams (1980; dashed line), Dill and Miller (1982; dash-dot line), and Smith (1996; thick solid line) (study locations from Uptegrove et al., 1995).....27
Figure 2-17. Map of U.S. Army Corps of Engineers (USACE) sand resource sites offshore Cape May County, New Jersey, and associated core locations (from Meisburger and Williams, 1980).....28
Figure 2-18. Isopach map illustrating sand ridge thickness at Inner Sand Ridge and Avalon Shoal (from Uptegrove et al., 1997). 30
Figure 2-19. Sediment thickness above the S_2 unconformity at Avalon Shoal. The bold line approximates the base of the sand ridge as it exists on top of the S_1 unconformity (from Smith, 1996). 31
Figure 2-20. Sand ridge volume as calculated using seismic data. Because sand ridge sediment thins away from the ridge crest, a bounding area was defined to calculate ridge thickness. The bounding area was defined by Smith (1996) as the 5-m contour above the regional S_2 boundary. The lower 2 m above the S_2 boundary was considered unusable, fine-grained, estuarine sediment based upon core observations. It was not included in the sand volume calculation (Smith, 1996).....32
Figure 2-21. Sediment thickness above the S_2 unconformity in the vicinity of Inner Sand Ridge (ISR). The surface expression of the inner ridge is approximated by the 5-m isopach, producing a sand volume estimate of approximately 48 MCM (from Smith, 1996).....33
Figure 2-22. Vibracore locations (yellow dots) for samples collected in 1997 at Sand Resource Areas C, G1, G2, G3, F1, and F2 (data from Alpine Ocean Seismic Survey, 1997). 34
Figure 2-23. Approximate locations of benthic sampling stations for previous biological surveys offshore New Jersey relative to the eight sand resource area locations (A1, A2, C1, F1, F2, G1, G2, G3). Numbers inside symbols indicate multiple stations. 40
Figure 2-24. Locations and average catches of hydraulic dredge hauls made during National Marine Fisheries Service surfclam/ocean quahog surveys (1977 to 1997) relative to the eight sand resource areas offshore New Jersey. 44
Figure 3-1. Changes in beach sediment volume and beach replenishment volume in Monmouth and Ocean Counties, New Jersey, 1986 to 1992 (from Uptegrove et al., 1995).....62
Figure 3-2. Changes in beach sediment volume and beach replenishment volume in Atlantic and Cape May Counties, New Jersey, 1986 to 1992 (from Uptegrove et al., 1995).....63
Figure 3-3. Shoreline position and change between Manasquan Inlet and Little Egg Inlet, New Jersey, 1839/40 to 1872/74.....67
Figure 3-4. Shoreline position and change between Manasquan Inlet and Little Egg Inlet, New Jersey, 1872/74 to 1899.....68
Figure 3-5. Shoreline position and change between Manasquan Inlet and Little Egg Inlet, New Jersey, 1899 to 1932.....69
Figure 3-6. Shoreline position and change between Brigantine Inlet and Hereford Inlet, New Jersey, 1841/42 to 1864/86.....70
Figure 3-7. Shoreline position and change between Brigantine Inlet and Hereford Inlet, New Jersey, 1864/86 to 1899.....71
Figure 3-8. Shoreline position and change between Brigantine Inlet and Hereford Inlet, New Jersey, 1899 to 1932.....72

Figure 3-9. Shoreline position and change between Manasquan Inlet and Little Egg Inlet, New Jersey, 1932 to 1950/51. 74
Figure 3-10. Shoreline position and change between Manasquan Inlet and Little Egg Inlet, New Jersey, 1950/51 to 1977. 75
Figure 3-11. Shoreline position and change between Brigantine Inlet and Hereford Inlet, New Jersey, 1932 to 1950/51. 76
Figure 3-12. Shoreline position and change between Brigantine Inlet and Hereford Inlet, New Jersey, 1950/51 to 1977. 77
Figure 3-13. Shoreline position and change between Manasquan Inlet and Little Egg Inlet, New Jersey, 1839/40 to 1977. 78
Figure 3-14. Shoreline position and change between Brigantine Inlet and Hereford Inlet, New Jersey, 1841/42 to 1977. 80
Figure 3-15. Nearshore bathymetry (1843/91) for offshore New Jersey. 83
Figure 3-16. Nearshore bathymetry (1934/77) for offshore New Jersey. 84
Figure 3-17. Nearshore bathymetry change (1843/91 to 1934/77) for the southeastern New Jersey shoreface. 86
Figure 3-18. Potential borrow site locations relative to sand ridge erosion and deposition in Resource Areas G1, G2, and G3. 88
Figure 3-19. Potential borrow site locations relative to sand ridge erosion and deposition in Resource Areas A1 and A2. 89
Figure 4-1. Comparison between spectral (REF/DIF S) and monochromatic (REF/DIF 1) wave models. Wave height results are compared to measured data (*) collected by Vincent and Briggs (1989). 92
Figure 4-2. Relative location of WIS stations and Reference Grids. 95
Figure 4-3. Twenty-year averaged wave rose for WIS Station Au2067. 98
Figure 4-4. Twenty-year averaged wave rose for WIS Station Au2069. 98
Figure 4-5. Twenty-year averaged wave rose for WIS Station Au2070. 99
Figure 4-6. Histogram plots of 20-year averaged peak periods and associated wave directions at WIS Station Au2067. The vertical bars are normalized by the greatest occurrence bin. 99
Figure 4-7. Histogram plots of 20-year averaged peak periods and associated wave directions at WIS Station Au2069. The vertical bars are normalized by the greatest occurrence bin. 100
Figure 4-8. Histogram plots of 20-year averaged peak periods and associated wave directions at WIS Station Au2070. The vertical bars are normalized by the greatest occurrence bin. 100
Figure 4-9. Illustration of reference grid notation (Kirby and Özkan, 1994). 106
Figure 4-10. Location of the four modeled reference grids along the New Jersey coastline. 107
Figure 4-11. Bathymetry for Reference Grid A, the defined sand resource areas, and the nearshore subgrid. 108
Figure 4-12. Bathymetry for Reference Grid B1, the defined sand resource areas, and the nearshore subgrid. 108
Figure 4-13. Bathymetry for Reference Grid B2, the defined sand resource areas, and the nearshore subgrid. 109
Figure 4-14. Bathymetry for Reference Grid C, the defined sand resource areas, and the nearshore subgrid. 109
Figure 4-15. Example of a rotated grid (Reference Grid A) to facilitate wave input. 110
Figure 4-16. Location of key bathymetric features within Grid A and location of proposed borrow site in Resource Areas A1 and A2. 112

Figure 4-17. Spectral wave modeling results for existing conditions using an eastern approach direction (0 degree bin) at reference Grid A. 113
Figure 4-18. Spectral wave modeling results for existing conditions using an east-southeast (-22.5 degree) approach direction at reference Grid A. 115
Figure 4-19. Spectral wave modeling results for existing conditions using an east-northeast (22.5 degree) approach direction at reference Grid A. 116
Figure 4-20. Spectral wave modeling results for existing conditions using a southeast (-45 degree) approach direction at reference Grid A. 118
Figure 4-21. Spectral wave modeling results for existing conditions using a south-southeastern (-67.5 degree) approach direction at reference Grid A. 119
Figure 4-22. Spectral wave modeling results for existing conditions simulating an estimated 50-yr northeast storm event for reference Grid A. 121
Figure 4-23. Spectral wave modeling results for existing conditions simulating an estimated 50-yr hurricane event for reference Grid A. 121
Figure 4-24. Wave height (green line, right-hand panel) taken from approximate breaker line (black line, left-hand panel) for the east (0 degree) approach simulation compared with historical shoreline change rates (black line, right-hand panel; 1864/86 to 1977). 122
Figure 4-25. Wave height (green line, right-hand panel) taken from the approximate breaker line (black line, left-hand panel) for combined directional approach simulations compared with shoreline change rates (black line, right-hand panel; 1864/86 to 1977). 124
Figure 4-26. Location of key bathymetric features within Grid B1 and location of proposed borrow site in Resource Area C1 125
Figure 4-27. Spectral wave modeling results for existing conditions using an eastern approach direction (0 degree bin) at Grid B1. 126
Figure 4-28. Spectral wave modeling results for existing conditions using an east-southeast (-22.5 degree) approach direction at Grid B1. 128
Figure 4-29. Spectral wave modeling results for existing conditions using an east-northeast (22.5 degree) approach direction at Grid B1. 129
Figure 4-30. Spectral wave modeling results for existing conditions using a southeast (-45 degree) approach direction at Grid B1. 131
Figure 4-31. Spectral wave modeling results for existing conditions using a south-southeast (-67.5 degree) approach direction at Grid B1. 132
Figure 4-32. Spectral wave modeling results for existing conditions simulating an estimated 50-yr northeast storm event at reference Grid B1 133
Figure 4-33. Spectral wave modeling results for existing conditions simulating an estimated 50-yr hurricane event at reference Grid B1 134
Figure 4-34. Wave height (green line, right-hand panel) taken from approximate breaker line (black line, left-hand panel) for the east (0 degree) approach simulation compared with historical shoreline change rates (black line, right-hand panel; 1864/68 to 1977). 135
Figure 4-35. Wave height (green line, right-hand panel) taken from approximate breaker line (black line, left-hand panel) for combined directional approach simulations compared with historic shoreline change rates (black line, right-hand panel; 1864/68 to 1977). 137
Figure 4-36. Location of key bathymetric features within Grid B2 and location of proposed dredge area G2 and G3 138
Figure 4-37. Spectral wave modeling results for existing conditions using an eastern approach direction (0 degree bin) at reference Grid B2. 139

Figure 4-38. Spectral wave modeling results for existing conditions using an east-southeast (-22.5 degree) approach direction for reference Grid B2. 140
Figure 4-39. Spectral wave modeling results for existing conditions using an east-northeast (22.5 degree) approach direction for reference Grid B2. 142
Figure 4-40. Spectral wave modeling results for existing conditions using a southeast (-45 degree) approach direction for reference Grid B2. 143
Figure 4-41. Spectral wave modeling results for existing conditions using a south-southeast (-67.5 degree) approach direction for reference Grid B2. 144
Figure 4-42. Spectral wave modeling results for existing conditions simulating an estimated 50-yr northeast storm event at reference Grid B2. 146
Figure 4-43. Spectral wave modeling results for existing conditions simulating an estimated 50-yr hurricane event at reference Grid B2. 146
Figure 4-44. Wave height (green line, right-hand panel) taken from the approximate breaker line location (black line, left-hand panel) for the east (0 degree) approach simulation compared with historic shoreline change (black line, right-hand panel; 1864/68 to 1977). 147
Figure 4-45. Wave height (green line, right-hand panel) taken from the approximate breaker line location(black line, left-hand panel) for combined directional approach simulations compared with historic shoreline change (black line, right-hand panel; 1864/68 to 1977). 149
Figure 4-46. Location of key bathymetric features within Grid C and location of the proposed borrow site in Resource Ares F2. 150
Figure 4-47. Spectral wave modeling results for existing conditions using an eastern approach direction (0 degree bin) for reference Grid C. 151
Figure 4-48. Spectral wave modeling results for existing conditions using an east-southeast (-22.5 degree) approach direction for reference Grid C. 152
Figure 4-49. Spectral wave modeling results for existing conditions using an east-northeast (22.5 degree) approach direction for reference Grid C. 154
Figure 4-50. Spectral wave modeling results for existing conditions using a northeastern (45 degree) approach direction for reference Grid C. 155
Figure 4-51. Spectral wave modeling results for existing conditions using a southeastern (-45 degree) approach direction for reference Grid C. 156
Figure 4-52. Spectral wave modeling results for existing conditions using a south-southeastern (-67.5 degree) approach direction for reference Grid C. 157
Figure 4-53. Spectral wave modeling results for existing conditions simulating an estimated 50-yr northeast storm event at reference Grid C. 158
Figure 4-54. Spectral wave modeling results for existing conditions simulating an estimated 50-yr hurricane event at reference Grid C. 159
Figure 4-55. Wave height (green line, left-hand center and right-hand panels) taken from approximate breaker line (black line, left-hand and right-hand center panels) for the east (0 degree) and east-southeast (-22.5 degree) approach simulations, compared with historical shoreline change rates (black line, left-hand center and right-hand panels; 1864/68 to 1977). 160
Figure 4-56. Wave height (green line, right-hand panel) taken from the approximate breaker line (black line, left-hand panel) for combined directional approach simulations compared with historical shoreline change rates (black line, right-hand panel; 1864/68 to 1977). 161
Figure 4-57. Spectral wave modeling results for post-dredging scenario using an eastern (0 degree) approach direction for reference Grid A. 162

Figure 4-58. Wave height modifications resulting from potential offshore mining at Sand Resource Areas A1 and A2 for the eastern (0 degree) approach simulation. Green shades identify areas of increased wave height, while blue shades identify areas of decreased wave height. 164
Figure 4-59. Wave height modifications resulting from potential offshore mining in Sand Resource Areas A1 and A2 for a 50-yr hurricane event. Green shades identify areas of increased wave height, while blue shades identify areas of decreased wave height. 166
Figure 4-60. Wave height modifications resulting from potential offshore sand borrow sites in Resource Areas A1 and A2 for a 50-yr northeast storm event. Green shades identify areas of increased wave height, while blue shades identify areas of decreased wave height. 166
Figure 4-61. Spectral wave modeling results for post-dredging scenario using an the eastern (0 degree) approach direction for reference Grid B1. 167
Figure 4-62. Wave height modifications resulting from potential offshore mining at the proposed sand borrow site in Resource Area C1 for the eastern (0 degree) approach simulation. Green shades identify areas of increased wave height, while blue shades identify areas of decreased wave height. 169
Figure 4-63. Wave height modifications resulting from potential offshore mining at the proposed borrow site in Resource Area C1 for a 50-yr hurricane event. Green shades identify areas of increased wave height, while blue shades identify areas of decreased wave height. 171
Figure 4-64. Wave height modifications resulting from potential offshore mining at the proposed borrow site in Resource Area C1 for the 50-yr northeast storm event. Green shades identify areas of increased wave height, while blue shades identify areas of decreased wave height. 171
Figure 4-65. Spectral wave modeling results for post-dredging scenario using an eastern (0 degree) approach direction for reference Grid B2. 172
Figure 4-66. Wave height modifications resulting from potential offshore mining at sand borrow sites in Resource Areas G1 through G3 for the eastern (0 degree) approach simulation. Green shades identify areas of increased wave height, while blue shades identify areas of decreased wave height. 174
Figure 4-67. Wave height modifications resulting from potential offshore sand mining in Resource Areas G2 top, G2 bottom, and G3 during a 50-yr hurricane event. Green shades identify areas of increased wave height, while blue shades identify areas of decreased wave height. 176
Figure 4-68. Wave height modifications resulting from potential offshore mining in Sand Resource Areas G1, G2 top, G2 bottom, and G3 for the 50-yr northeast storm event. Green shades identify areas of increased wave height, while blue shades identify areas of decreased wave height. 176
Figure 4-69. Spectral wave modeling results for post-dredging scenario using an eastern (0 degree) approach direction for reference Grid C. 177
Figure 4-70. Wave height modifications resulting from potential offshore sand mining at Resource Area F2 for the eastern (0 degree) approach simulation. Green shades identify areas of increased wave height, while blue shades identify areas of decreased wave height. 179
Figure 4-71. Wave height modifications resulting from potential offshore sand mining in Resource Area F2 a 50-yr hurricane event. Green shades identify areas of increased wave height, while blue shades identify areas of decreased wave height. 181

Figure 4-72. Wave height modifications resulting from potential offshore sand mining in Resource Area F2 for the 50-yr northeast storm event. Green shades identify areas of increased wave height, while blue shades identify areas of decreased wave height. 181
Figure 5-1. Histogram showing the relative energy (variance) of separated current processes: tides, high frequency, wind-driven, and low-frequency flows. Units are $(cm/sec)^2$. Along-shelf wind-driven flows in winter were the most energetic current component. 188
Figure 5-2. Time series of individual along-shelf flow processes for February-March (Winter) 1994. Note the strong wind-driven currents that occurred in late February. These strong currents likely resulted from either a storm (local wind response) or freely-propagating waves. In either case, wind-driven currents account for most of the along-shelf signal. 189
Figure 5-3. Time series of individual cross-shelf flow processes for February-March (Winter) 1994. Note the lack of wind-driven currents in late February, when the along-shelf flow (Figure 5-2) showed noticeable variability. Semi-diurnal tides account for most of the cross-shelf signal. 190
Figure 5-4. Shallow water and deep water wave orbits. 192
Figure 5-5. Schematic of wave-induced bottom velocities. 193
Figure 5-6. Schematic longshore velocity profiles with and without cross-shore mixing (the abrupt reduction in velocity for the without mixing case occurs at the breaker line). 196
Figure 5-7. Comparison of model and observed longshore current velocities from field measurements taken by Kraus and Sasaki (1979). 199
Figure 5-8. Comparison of modeled to observed longshore current velocities from field measurements taken by Thornton and Guza (1989). 199
Figure 5-9. S_{xy} radiation stress and maximum longshore current velocities predicted by the wave-induced current model within Grid A for the -22.5° wave condition. Positive velocities are toward the south. 201
Figure 5-10. Longshore current profiles along selected transects within Grid A for the -22.5° wave condition (colored transects in the left sub-plot correspond to like colored profiles in the right sub-plot). 202
Figure 5-11. Location of the offshore observation regions within Sand Resource Areas A1 and areas A2. These observation areas were used to determine potential sediment transport at borrow sites following numerical dredging. 204
Figure 5-12. Location of the offshore observation regions within Sand Resource Area C1. These observation areas were used to determine potential sediment transport at the borrow sites following numerical dredging. 205
Figure 5-13. Location of the offshore observation regions within Sand Resource Areas G2 Top, G2 Bottom, and G3. These observation areas were used to determine potential sediment transport at the borrow sites following numerical dredging. 206
Figure 5-14. Location of the offshore observation regions within Sand Resource Area F2. These observation areas were used to determine potential sediment transport at the borrow sites following numerical dredging. 206
Figure 5-15. East-Northeast (22.5°) influenced hydrodynamic and sediment transport results at Sand Resource Area A1. 208
Figure 5-16. East (0°) influenced hydrodynamic and sediment transport results at Sand Resource Area A1. 208

Figure 5-17. East-Southeast (-22.5°) influenced hydrodynamic and sediment transport results at Sand Resource Area A1. 209
Figure 5-18. Southeast (-45°) influenced hydrodynamic and sediment transport results at Sand Resource Area A1. 209
Figure 5-19. South-Southeast (-67.5°) influenced hydrodynamic and sediment transport results at Sand Resource Area A1. 210
Figure 5-20. East-Northeast (22.5°) influenced hydrodynamic and sediment transport results at Sand Resource Area A2. 211
Figure 5-21. East (0°) influenced hydrodynamic and sediment transport results at Sand Resource Area A2. 211
Figure 5-22. East-Southeast (-22.5°) influenced hydrodynamic and sediment transport results at Sand Resource Area A2. 212
Figure 5-23. Southeast (-45°) influenced hydrodynamic and sediment transport results at Sand Resource Area A2. 212
Figure 5-24. South-Southeast (-67.5°) influenced hydrodynamic and sediment transport results at Sand Resource Area A2. 213
Figure 5-25. East-northeast influenced hydrodynamic and sediment transport results at Sand Resource Area C1. 215
Figure 5-26. East influenced hydrodynamic and sediment transport results at Sand Resource Area C1. 216
Figure 5-27. East-southeast influenced hydrodynamic and sediment transport results at Sand Resource Area C1. 216
Figure 5-28. Southeast influenced hydrodynamic and sediment transport results at Sand Resource Area C1. 217
Figure 5-29. South southeast hydrodynamic and sediment transport results at Sand Resource Area C1. 217
Figure 5-30. East-northeast (22.5°) influenced hydrodynamic and sediment transport results at Sand Resource Area G2 Top. 219
Figure 5-31. East-northeast (22.5°) influenced hydrodynamic and sediment transport results at Sand Resource Area G2 Bottom. 220
Figure 5-32. East-northeast (22.5°) influenced hydrodynamic and sediment transport results at Sand Resource Area G3. 220
Figure 5-33. East (0°) influenced hydrodynamic and sediment transport results at Sand Resource Area G2 Top. 221
Figure 5-34. East (0°) influenced hydrodynamic and sediment transport results at Sand Resource Area G2 Bottom. 221
Figure 5-35. East (0°) influenced hydrodynamic and sediment transport results at Sand Resource Area G3. 222
Figure 5-36. East-southeast (-22.5°) influenced hydrodynamic and sediment transport results at Sand Resource Area G2 Top. 222
Figure 5-37. East-southeast (-22.5°) influenced hydrodynamic and sediment transport results at Sand Resource Area G2 Bottom. 223
Figure 5-38. East-southeast (-22.5°) influenced hydrodynamic and sediment transport results at Sand Resource Area G3. 223
Figure 5-39. Southeast (-45°) influenced hydrodynamic and sediment transport results at Sand Resource Area G2 Top. 224
Figure 5-40. Southeast (-45°) influenced hydrodynamic and sediment transport results at Sand Resource Area G2 Bottom. 224

Figure 5-41. Southeast (-45°) influenced hydrodynamic and sediment transport results at Sand Resource Area G3. 225
Figure 5-42. South-southeast (-67.5°) influenced hydrodynamic and sediment transport results at Sand Resource Area G2 Top. 225
Figure 5-43. South-southeast (-67.5°) influenced hydrodynamic and sediment transport results at Sand Resource Area G2 Bottom. 226
Figure 5-44. South-southeast (-67.5°) case hydrodynamic and sediment transport results at Sand Resource Area G3. 226
Figure 5-45. Northeast (45°) influenced hydrodynamic and sediment transport results at Sand Resource Area F2. 228
Figure 5-46. East-northeast (22.5°) influenced hydrodynamic and sediment transport results at Sand Resource Area F2. 229
Figure 5-47. East (0°) influenced hydrodynamic and sediment transport results at Sand Resource Area F2. 229
Figure 5-48. East-southeast (-22.5°) influenced hydrodynamic and sediment transport results at Sand Resource Area F2. 230
Figure 5-49. Southeast (-45°) influenced hydrodynamic and sediment transport results at Sand Resource Area F2. 230
Figure 5-50. South-southeast (-67.5°) influenced hydrodynamic and sediment transport results at Sand Resource Area F2. 231
Figure 5-51. Map showing the various Grids used for wave-induced current and longshore sediment transport potential modeling. 235
Figure 5-52. S_{xy} radiation stress values and annualized sediment transport potential for the –22.5° wave condition within Grid A. 237
Figure 5-53. Gross and net annual longshore sediment transport potential for Grid A. 239
Figure 5-54. Gross and net annual longshore sediment transport potential for Grid B2. 240
Figure 5-55. Gross and net annual longshore sediment transport potential for Grid B1. 241
Figure 5-56. S_{xy} radiation stress values and annualized sediment transport potential for the –22.5° wave condition within Grid C. 242
Figure 5-57. Longshore sediment transport potential for 50-year hurricane condition at Grid B2. 244
Figure 5-58. Longshore sediment transport potential for 50-year hurricane condition at Grid B1. 245
Figure 5-59. Cross-shore distribution of longshore current and sediment transport for three selected transects for the –22.5° wave condition within Grid A. 246
Figure 5-60. Annual longshore sediment transport potential, normalized change in longshore transport (modeled accretion/erosion potential), and observed shoreline change between 1899 and 1977 for Grid A. 247
Figure 5-61. Annual longshore sediment transport potential, normalized change in longshore transport (modeled accretion/erosion potential), and observed shoreline change between 1899 and 1977 for Grid B2. 248
Figure 5-62. Annual longshore sediment transport potential, normalized change in longshore transport (modeled accretion/erosion potential), and observed shoreline change between 1899 and 1977 for Grid B1. 249
Figure 5-63. Annual longshore sediment transport potential for the –22.5° wave condition, normalized change in longshore transport (modeled accretion/erosion potential), and observed shoreline change between 1899 and 1977 for Grid C. 250
Figure 6-1. Adjacent stations relative to the eight sand resource areas and the New Jersey coast. 254

Figure 6-2. Sampling locations for New Jersey Sand Resource Area A1.....257
Figure 6-3. Sampling locations for New Jersey Sand Resource Area A2.....258
Figure 6-4. Sampling locations for New Jersey Sand Resource Area C1. 259
Figure 6-5. Sampling locations for New Jersey Sand Resource Area F1.....260
Figure 6-6. Sampling locations for New Jersey Sand Resource Area F2.....261
Figure 6-7. Sampling locations for New Jersey Sand Resource Area G1. 262
Figure 6-8. Sampling locations for New Jersey Sand Resource Area G2. 263
Figure 6-9. Sampling locations for New Jersey Sand Resource Area G3. 264
Figure 6-10. Temperature and salinity water column profiles from Resource Areas A1, A2, C1, F2, G2, and G3 during the May 1998 Survey 1 offshore New Jersey. 270
Figure 6-11. Temperature and dissolved oxygen water column profiles from Resource Areas A1, A2, C1, F2, G2, and G3 during the May 1998 Survey 1 offshore New Jersey. 271
Figure 6-12. Temperature and salinity water column profiles from Resource Areas A1, A2, C1, F2, G1, G2 and G3 during the September 1998 Survey 2 offshore New Jersey. 272
Figure 6-13. Temperature and dissolved oxygen water column profiles from Resource Areas A1, A2, C1, F2, G1, G2, and G3 during the September 1998 Survey 2 offshore New Jersey.....273
Figure 6-14. Station groups (A to F; X and Y) based on normal cluster analysis of infaunal samples collected during the May 1998 Survey 1 and September 1998 Survey 2 in the eight sand resource areas (A1, A2, C1, F1, F2, G1, G2, and G3) and three adjacent stations offshore New Jersey. 281
Figure 6-15. Grain size composition of infaunal samples collected during the May 1998 Survey 1 (S1) and September 1998 Survey 2 (S2) in the eight sand resource areas offshore New Jersey. Sample order and groups (A to F; X and Y) are based on normal cluster analysis. 282
Figure 7-1. Difference in annual transport rates associated with dredging sand borrow sites for the –22.5º wave condition at Grid B1. The UTM Northing coordinate limits of the potential borrow site are shown with thick lines.....312
Figure 7-2. Difference in average annual transport rates associated with dredging sand borrow sites for Grid A. 314
Figure 7-3. Difference in average annual transport rates associated with dredging sand borrow sites for Grid B2. 315
Figure 7-4. Difference in average annual transport rates associated with dredging sand borrow site for Grid B1. 317
Figure 7-5. Difference in average transport rate for the –22.5º wave condition associated with dredging sand borrow site for Grid C. 318
Figure 7-6. Difference in annualized transport rate for northeast storm wave condition associated with dredging sand borrow sites for Grid A. 320
Figure 7-7. Difference in annualized transport rate for the hurricane wave condition associated with dredging sand borrow sites for Grid A. 321
Figure 7-8. Difference in annualized transport rate for northeast storm condition associated with dredging the sand borrow site for Grid B1. 322
Figure 7-9. Difference in annualized transport rate for the hurricane wave condition associated with dredging the sand borrow site for Grid B1. 323

LIST OF TABLES

Table 1-1. Sand Resource Characteristics at Potential Borrow Sites in Resource Areas Offshore New Jersey....4
Table 1-2. UTM Coordinates defining borrow site polygons offshore New Jersey....5
Table 2-1. Geological studies documenting Holocene sedimentation processes on the New Jersey continental shelf (after Uptegrove et al., 1995)....22
Table 2-2. Seasonal variations in mean abundance (#/m^3) of zooplankton in the New York Bight, 1974 to 1975 (after: Judkins et al., 1980)....48
Table 2-3. Summary of spawning times and location of fishes in the central part of the Middle Atlantic Bight (after: Able and Fahay, 1998)....50
Table 2-4. Ranking of the most abundant larval fishes collected in continental shelf waters in the central part of the Middle Atlantic Bight during Marine Monitoring, Assessment and Prediction Program (MARMAP) surveys from 1977 to 1987 (after: Able and Fahay, 1998)....52
Table 3-1. Summary of shoreline source data characteristics for the New Jersey coast between Manasquan Inlet and Hereford Inlet....64
Table 3-2. Estimates of potential error associated with New Jersey shoreline position surveys....65
Table 3-3. Maximum root-mean-square potential error for New Jersey shoreline change data....65
Table 3-4. Summary of bathymetry source data characteristics for the offshore area between Manasquan Inlet and Cape May, New Jersey....81
Table 4-1. Summary of relevant WIS stations in the modeling domain....94
Table 4-2. Inventory of relevant observation stations....95
Table 4-3. Input conditions used for comparison of WIS and LEO-15 data....96
Table 4-4. Test simulation results for comparison of WIS and LEO-15 data....96
Table 4-5. Summary of the directional bin breakdown of the Au2067 WIS station data....101
Table 4-6. Summary of the directional bin breakdown of the Au2069 WIS station data....101
Table 4-7. Summary of the directional bin breakdown of the Au2070 WIS station data....101
Table 4-8. Return periods from results of Gumbel Distribution Hindcast (USACE, 1997)....102
Table 4-9. Wave transformation numerical modeling input conditions and scenarios for Grid A....105
Table 4-10. Wave transformation numerical modeling input conditions and scenarios for Grid B2....105
Table 4-11. Wave transformation numerical modeling input conditions and scenarios for Grid B1....105
Table 4-12. Wave transformation numerical modeling input conditions and scenarios for Grid C....105
Table 4-13. Reference grid dimensions....107
Table 4-14. Subgrid dimensions....111
Table 4-15. Dredged depth and resulting sand volume within respective sand resource area....111
Table 4-16. Coastline areas experiencing increased wave heights during eastern wave approach....114

Table 4-17. Coastline areas experiencing increased wave heights during east-southeast wave approach. 116
Table 4-18. Coastline areas experiencing increased wave heights during east-northeast wave approach. 117
Table 4-19. Coastline areas experiencing increased wave heights during southeastern wave approach. 118
Table 4-20. Coastline areas experiencing increased wave heights during south-southeastern wave approach. 120
Table 4-21. Percent occurrence weighting for simulated directional approach bins to reconstruct an approximate annual average for Grid A. 123
Table 4-22. Coastline areas experiencing increased wave heights during eastern wave approach at Grid B1. 127
Table 4-23. Coastline areas experiencing increased wave heights during east-southeast wave approach at Grid B1. 128
Table 4-24. Coastline areas experiencing increased wave heights during east-northeast wave approach at Grid B1. 129
Table 4-25. Coastline areas experiencing increased wave heights during southeast wave approach at Grid B1. 130
Table 4-26. Coastline areas experiencing increased wave heights during south-southeastern wave approach at Grid B1. 132
Table 4-27. Percent occurrence weighting for simulated directional approach bins to reconstruct an approximate annual average wave climate for Grid B1. 136
Table 4-28. Coastline areas experiencing increased wave heights during eastern wave approach at Grid B2. 140
Table 4-29. Coastline areas experiencing increased wave heights during east-southeastern wave approach at Grid B2. 141
Table 4-30. Coastline areas experiencing increased wave heights during east-northeast wave approach at Grid B2. 142
Table 4-31. Coastline areas experiencing increased wave heights during southeastern wave approach at Grid B2. 143
Table 4-32. Coastline areas experiencing increased wave heights during south-southeast wave approach at Grid B2. 144
Table 4-33. Percent occurrence weighting for simulated directional approach bins to reconstruct an approximate annual average wave climate for Grid B2. 148
Table 4-34. Coastline areas experiencing increased wave heights during eastern wave approach at Grid C. 152
Table 4-35. Coastline areas experiencing increased wave heights during east-southeast wave approach at Grid C. 153
Table 4-36. Coastline areas experiencing increased wave heights during east-northeastern wave approach at Grid C. 153
Table 4-37. Coastline areas experiencing increased wave heights during northeast wave approach at Grid C. 154
Table 4-38. Coastline areas experiencing increased wave heights during southeast wave approach at Grid C. 155
Table 4-39. Coastline areas experiencing increased wave heights during south-southeast wave approach at Grid C. 157
Table 4-40. Percent occurrence weighting for simulated directional approach bins to reconstruct an approximate annual average for Grid C. 161
Table 4-41. Coastline regions impacted by potential offshore dredging in Resource Areas A1 and A2. 165

Table 4-42. Coastline regions impacted by the potential offshore dredging of Resource Area C1. 170
Table 4-43. Coastal regions impacted by the potential offshore dredging in Resource Areas G2 top, G2 bottom, and G3. 175
Table 4-44. Coastal regions impacted by the potential offshore dredging of Resource Area F2. 180
Table 5-1. Sediment sizes at Sand Resource Areas A1 through G3. 205
Table 5-2. Percent contributed based on energy per bin. 207
Table 5-3. Sediment Transport Summary for Areas A1 and A2 214
Table 5-4. Sediment Transport Summary for Resource Area C1 218
Table 5-5. Sediment Transport Summary for Grid B2 227
Table 5-6. Sediment Transport Summary for F2 231
Table 5-7. Summary of directional-averaged (including calm seas) sediment transport results and estimated infilling times. 232
Table 6-1. Sampling for the New Jersey May 1998 Survey 1 and September 1998 Survey 2. Where number of samples planned differ from number of samples collected, number of samples collected are given in parentheses. 255
Table 6-2. Ten most abundant infaunal taxa from samples collected during the May 1998 Survey 1 in the eight resource areas (A1, A2, C1, F1, F2, G1, G2, and G3) and three adjacent stations (R1, R2, and R3) offshore New Jersey. 275
Table 6-3. Ten most abundant infaunal taxa from samples collected during the September 1998 Survey 2 in the eight sand resource areas (A1, A2, C1, F1, F2, G1, G2, and G3) and three adjacent stations (R1, R2, and R3) offshore New Jersey. 277
Table 6-4. Summary of infaunal statistics by survey for sand resource areas (A1, A2, C1, F1, F2, G1, G2, and G3) and adjacent stations (R1, R2, and R3) offshore New Jersey. 278
Table 6-5. Occurrence and density of juvenile Atlantic surfclam, *Spisula solidissima*, in Smith-McIntyre grab samples taken in the eight sand resource areas and three adjacent stations during the May 1998 Survey 1 and September 1998 Survey 2 offshore New Jersey. 280
Table 6-6. Infaunal species groups resolved from inverse cluster analysis of all samples collected during the May 1998 Survey 1 and September 1998 Survey 2 in the eight sand resource areas and three adjacent stations offshore New Jersey. 283
Table 6-7. Two-way table from normal (Station Groups A-D) and inverse (Species Groups 1-3[a]) cluster analysis of infaunal samples collected during the May 1998 Survey 1 (S1) and September 1998 Survey 2 (S2) in Sand Resource Area A1 offshore New Jersey. Data are presented as total counts for individual taxa. 285
Table 6-8. Two-way table from normal (Station Groups A-C) and inverse (Species Groups 1-4[a]) cluster analysis of infaunal samples collected during the May 1998 Survey 1 (S1) and September 1998 Survey 2 (S2) in Sand Resource Area A2 offshore New Jersey. Data are presented as total counts for individual taxa. 287
Table 6-9. Two-way table from normal (Station Groups A-E) and inverse (Species Groups 1 and 2[a]) cluster analysis of infaunal samples collected during the May 1998 Survey 1 (S1) and September 1998 Survey 2 (S2) in Sand

Resource Area C1 offshore New Jersey. Data are presented as total counts for individual taxa 288
Table 6-10. Two-way table from normal (Station Groups A and B) and inverse (Species Groups 1 and 2[a]) cluster analysis of infaunal samples collected during the May 1998 Survey 1 (S1) and September 1998 Survey 2 (S2) in Sand Resource Area F1 offshore New Jersey. Data are presented as total counts for individual taxa. 290
Table 6-11. Two-way table from normal (Station Groups A and B) and inverse (Species Groups 1 and 2[a]) cluster analysis of infaunal samples collected during the May 1998 Survey 1 (S1) and September 1998 Survey 2 (S2) in Sand Resource Area F2 offshore New Jersey. Data are presented as total counts for individual taxa. 291
Table 6-12. Two-way table from normal (Station Groups A-E) and inverse (Species Groups 1-4[a]) cluster analysis of infaunal samples collected during the May 1998 Survey 1 (S1) and September 1998 Survey 2 (S2) in Resource Area G1 offshore New Jersey. Data are presented as total counts for individual taxa. 293
Table 6-13. Two-way table from normal (Station Groups A-C) and inverse (Species Groups 1-3[a]) cluster analysis of infaunal samples collected during the May 1998 Survey 1 (S1) and September 1998 Survey 2 (S2) in Sand Resource Area G2 offshore New Jersey. Data are presented as total counts for individual taxa. 294
Table 6-14. Two-way table from normal (Station Groups A-C) and inverse (Species Groups 1-4[a]) cluster analysis of infaunal samples collected during the May 1998 Survey 1 (S1) and September 1998 Survey 2 (S2) in Sand Resource Area G3 offshore New Jersey. Data are presented as total counts for individual taxa. 296
Table 6-15. Epifauna and demersal fishes collected by mongoose trawl and ranked by numerical abundance from the May 1998 Survey 1 at six potential sand resource areas offshore New Jersey. 298
Table 6-16. Epifauna and demersal fishes collected by mongoose trawl and ranked by numerical abundance form the September 1998 Survey 2 at seven potential sand resource areas offshore New Jersey 299
Table 6-17. Two-way table from normal (Station Groups A and B) and inverse (Species Groups 1-4) cluster analysis of trawl samples collected during the May 1998 Survey 1 (S1) and September 1998 Survey 2 (S2) from sand resource areas (A1, A2, C1, F2, G1, G2, and G3) offshore New Jersey. Data are presented as total counts for individual taxa. 301
Table 7-1. Statistical parameters for annual average sediment transport conditions associated with Sub-Grids A, B2, B1, and C. 324
Table 7-2. Invertebrate and fish species for which Essential Fish Habitat has been identified in the vicinity of the eight sand resource areas offshore New Jersey (adapted from Mid-Atlantic Fishery Management Council, 1998a,b,c,d, 1999; New England Fishery Management Council, 1998a,b; National Marine Fisheries Service, 1999). 343

LIST OF ABBREVIATIONS

μ	micron
ACI	Aubrey Consulting, Inc.
ASTM	American Society for Testing Materials
BVA	Barry Vittor & Associates, Inc.
CEQ	Council on Environmental Quality
CERC	Coastal Engineering Research Center
CETAP	Cetacean and Turtle Assessment Program
CHL	Coastal Hydraulics Laboratory
cm	centimeter
CRC	Coastal Research Center
CSA	Continental Shelf Associates, Inc.
DEC	Division of Engineering and Construction
DGPS	Differential Global Positioning System
EA	Environmental Assessment
EEZ	Exclusive Economic Zone
EFH	Essential Fish Habitat
EIS	Environmental Impact Statement
ESA	Endangered Species Act
FMP	Fishery Management Plan
ft	feet
ha	hectare
INTERMAR	International Activities and Marine Minerals Division
km	kilometers
kts	knots
LEO	Long-Term Ecosystem Observatory
LPIL	Lowest Practical Identification Level
m	meter
MAB-NURC	Mid-Atlantic Bight National Undersea Research Center
MAFMC	Mid-Atlantic Fisheries Management Council
MARMAP	Marine Monitoring, Assessment, and Prediction Program
MCM	million cubic meters
MCY	million cubic yards
mi	statute mile
mm	millimeter
MMS	Minerals Management Service
MSL	Mean Sea Level
MWL	Mean Water Level
NAD	North American Datum
NEFMC	New England Fisheries Management Council
NEPA	National Environmental Policy Act
NGDC	National Geophysical Data Center
NGVD	National Geodetic Vertical Datum
NJDEP	New Jersey Department of Environmental Protection
NJGS	New Jersey Geological Survey
NMFS	National Marine Fisheries Service
NOAA	National Oceanic and Atmospheric Administration
OCS	Outer Continental Shelf
OCSLA	Outer Continental Shelf Lands Act
ODFS	Offshore Demersal Fishing Sampling
Ppt	parts per thousand
REF/DIF S	Refraction/Diffraction Model for Spectral Wave Conditions
sec	second
USACE	U.S. Army Corps of Engineers
USC & GS	U.S. Coast and Geodetic Survey
USDOI	U.S. Department of the Interior
USFWS	U.S. Fish and Wildlife Service
UTM	Universal Transverse Mercator
WIS	Wave Information Study
WISWAVE	Wave Information Study Wave Model
yd	yard
yr	year